Addendum to the proposal "A Fast Track Trigger with High Resolution for H1"

H1 Collaboration

September 20, 1999

1 Preface

In June this year, it was proposed to instrument the H1 experiment with a high resolution Fast Track Trigger (FTT) [1]. Considerable progress has been made with the project since then. Improvements have been made in the simulation software, allowing updated and more detailed studies of the expected FTT performance. Investigations have been made in which the essential parameters of the central jet chamber (CJC) performance have been varied to check the robustness of the proposed trigger in the case of severe running conditions. For the most important physics topics, the gain in statistics offered by the FTT and its systematic limitations have been quantified. With these results in hand we are now able to predict more precisely the behaviour and physics yield of the FTT after the HERA machine upgrade.

This note summarises the new results and answers the questions raised by the PRC concerning the motivation, construction, and operation of the FTT. Section 2 elaborates on the physics motivation for building the FTT. In section 3 the improvements in precision that the FTT will yield for HERA physics are quantified. Technical issues related to the performance of the device are discussed in section 4. Finally, an updated overview of the tasks and responsibilities of the project is given in section 5.

2 Heavy Flavour Physics beyond the Upgrade

The prospects for physics in the absence of very high transverse momentum particles at the upgraded HERA were discussed in section 3.1 of [1]. The triggering problem without a FTT was explained in section 3.2. Here, we provide additional information on the more important items, in particular those related to heavy flavour physics.

2.1 Charm Physics

The unique heavy flavour physics opportunities provided by the upgraded HERA lie in the improvement of our understanding of QCD. It may also be possible for HERA to make contributions to charm physics itself (e.g. through measurements of fragmentation functions or searches for rare decay modes). Although the overall

charm yields are unlikely to be large enough to seriously compete with other experiments in this regard, HERA provides an environment for such studies that is complementary to those available elsewhere.

It has already been shown that the contribution of events containing charm is very large at low x at HERA. The fraction $F_2^{c\bar{c}}/F_2$ of charmed final states varies between approximately 10% at $Q^2 \sim 1\ \mathrm{GeV}^2$ and 30% at $Q^2 \sim 100\ \mathrm{GeV}^2$ [2, 3]. A correct treatment of the charm contribution is therefore an essential ingredient of any QCD model of low x HERA data. However, only a small fraction of the charm yield is observable, due to the very low branching ratios to detectable channels. Much larger luminosities are required in order to test the treatment of charm directly in the data to the precision required for models of F_2.

The proper way to deal with charm (and beauty) production in DIS is a largely unanswered question in QCD. The presence of a second hard scale arising from the charm quark mass m_c leads to problems in the convergence properties of perturbative series, which contain terms of the form $\ln Q^2/m_c^2$. For $Q^2 \sim m_c^2$, the generally accepted procedure is to produce charm entirely via the boson-gluon fusion (BGF) process $\gamma^* g \rightarrow c\bar{c}$, the initial state proton containing only light (u, d, s) quarks. Where $Q^2 \gg m_c^2$, charm is usually treated as a fourth flavour in the proton sea with zero mass, evolving in the same manner as the light quarks. Several competing models exist for the merging of the two schemes at intermediate Q^2 [4, 5]. High precision charm data are required to provide a testing ground to distinguish between these different possible procedures.

Since charm production proceeds dominantly via boson-gluon fusion at HERA, charm data are sensitive to the gluon distribution, which heavily dominates proton structure at low x. The best results on the parton distributions of the proton come from global fits to a variety of data [5]. Except at the highest values of x, the gluon distribution in these fits is basically derived from inclusive deep-inelastic scattering data, essentially through the scaling violations of $F_2(x, Q^2)$ [6]. However, such fits are dependent on the use of the DGLAP QCD evolution equations [7] and are relatively insensitive to any failure in the underlying theoretical framework, for example, due to the effects of BFKL dynamics [8] at low x.

The most attractive direct methods of obtaining the gluon distribution of the proton are by studying dijet events and charm production in DIS by the BGF process. Matters are complicated in the case of dijet production by the background to BGF arising from the QCD-Compton process $\gamma^* q \rightarrow qg$. In addition, large values of x are kinematically required in order to produce high transverse momentum jet pairs, restricting the kinematic region in which the gluon distribution can be extracted. Charm measurements thus provide the cleanest direct means of extracting the gluon distribution of the proton and explore a larger kinematic region than is possible from dijet production. At the very least, charm data provide an important test of the QCD factorisation theorem, which implies that the gluon distributions extracted from charm data and from fits to F_2 data should be identical. At best, charm data could identify deficiencies of the theory in the low x region.

By studying particular types of final state, the gluon distributions of the photon and pomeron can also be measured. Here, there is little alternative to direct means of extraction of gluon distributions. HERA dijet data already provide the best constraints on real photon structure at low x and on virtual photon structure throughout the kinematic phase space [9]. With better statistics, similar analysis of charm events will be possible. In diffractive scattering, the gluon distribution of the pomeron, as extracted from QCD fits to the diffractive DIS cross section, has very large uncertainties [10]. Despite the poor statistics, hadronic final state measurements are already proving competitive in their sensitivity to the pomeron gluon distribution [11, 12].

2.2 Beauty Physics

The study of beauty production at HERA has barely begun, due to the very low production cross sections. However, with sufficient statistics, all of the planned programme of charm physics is equally applicable to beauty. It is very interesting that the first HERA measurements in the beauty sector [13] reveal cross sections that are substantially larger than those predicted in the low orders of QCD. By contrast, despite some disagreements

in differential distributions, the overall charm cross section is consistent with predictions [2]. It is essential to obtain much larger samples of beauty events in order to investigate whether this apparent discrepancy is merely a statistical fluctuation or whether there are real deficiencies in the theory. Since the cross section is heavily dominated by photoproduction, it will be crucial to trigger events at the lowest Q^2 if useful statistics are to be collected. After the upgrade, it will certainly not be possible to trigger beauty (or charm) events in photoproduction without the FTT, as rates will certainly be prohibitive. With the FTT, a coincidence of a D^* candidate in the central tracker and and an electron in one of the low angle taggers [1] would give an acceptable rate (see section 3.2).

The prospects for triggering beauty events with the FTT after the upgrade have been investigated using a sample of simulated $\gamma^* p \rightarrow b\bar{b}$ events in which exactly one D^* meson is reconstructed, originating from the decays of the b hadrons. The kinematic range studied [2] is $2 < Q^2 < 100\ \mathrm{GeV}^2$ and $10^{-3} < x_g < 10^{-1}$. As usual, the trigger is based on cuts in the reconstructed D^0 mass and $\Delta M = M(D^*) - M(D^0)$ for the decay chain $D^* \rightarrow D^0 \pi_{\mathrm{slow}} \rightarrow K\pi\pi_{\mathrm{slow}}$. The efficiency with which the D^* meson is triggered by the FTT is shown in figure 1. The results from another simulated file with D^* mesons produced directly from a charm quark in the process $\gamma^* p \rightarrow c\bar{c}$ are shown for comparison.

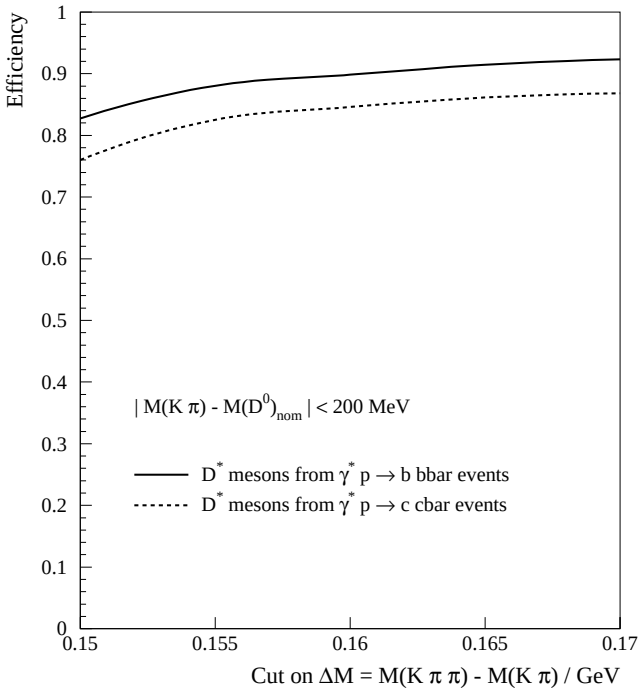

Figure 1: Estimated efficiencies for D^* mesons in DIS using the proposed trigger for $|M(K\pi) - M(D^0)| < 200\ \mathrm{MeV}$ and various choices of cut on ΔM. The efficiencies are relative to a sample of simulated events in which the selection criteria on the polar angles and transverse momenta of the D^* and its decay products of [2] are applied. A comparison is made between D^* mesons produced directly in the process $\gamma^* p \rightarrow c\bar{c}$ and those produced as part of the decay chain following the hard process $\gamma^* p \rightarrow b\bar{b}$.

Figure 1 demonstrates that the efficiency for triggering D^* mesons in $b\bar{b}$ events is slightly better than that for $c\bar{c}$ events. The main reason for this is the higher transverse momentum and higher centrality of D^* mesons and their decay products in $b\bar{b}$ than in $c\bar{c}$ events (see figure 2 of the original proposal). Losses due to the shift in the D^* decay vertex with respect to the overall event vertex are negligible, since the beauty hadrons are always

[1] The HERA upgrade will require changes to the H1 low angle electron taggers. However, with a new tagger $6\ \mathrm{m}$ downstream and an existing tagger $44\ \mathrm{m}$ downstream, the acceptances for photoproduction processes are expected to be similar to those before the upgrade [14] .

[2] DIS events only have been studied to date. However, no major differences in efficiency are expected in the photoproduction regime.

produced near threshold at HERA and the vertex information available to the FTT is not sufficiently precise to be sensitive to such vertex shifts. The results of this study are highly encouraging for the study of b physics after the upgrade, especially if the FTT can be used in conjunction with the central silicon tracker CST (see section 2.3).

2.3 Relation to the Central Silicon Tracker

Work with the CST continues in earnest and analysis of existing data is well underway. However, statistics are limited thus far and the increased luminosities available after the upgrade will be crucial if the device is fully to be exploited.

Although silicon micro-vertex detectors provide a means of obtaining very high purity heavy flavour samples, it is not always possible to identify the secondary vertex and overall efficiencies are relatively low for both charm and beauty tagging. HERA is at a disadvantage in beauty physics using silicon detectors compared for example to LEP. This is mainly because the product of the Lorentz factors $\beta\gamma$ is typically rather small, such that the distance between the principal and secondary vertices is also usually small. With additional complications due to multiple scattering, it is clear that other means of identifying heavy flavour physics are, and will always be, necessary to complement the CST data.

It is not technically possible to use the CST itself to provide a trigger, since on-line track reconstruction is not available and the CST consists of only two layers, which does not provide sufficient redundancy. Triggering events containing heavy flavour signatures in the CST is already problematic with the existing H1 trigger set-up. This situation will become much worse after the HERA upgrade, when trigger conditions will become much tighter. The FTT will thus naturally fulfil the role of triggering a large fraction of the events that are of interest for CST studies. The most likely scenario after the upgrade is that events triggered by the FTT on the basis of a charmed meson will form a starting sample for CST analysis. Without a FTT, heavy flavour events of interest for CST analysis will be downscaled randomly along with all other events that do not contain high transverse momentum signatures.

3 Physics Yields with the FTT

3.1 Expected Yields Before and After the Upgrade

Typically, H1 has so far published measurements of processes of relevance to the FTT using data collected up to 1996. Analysis of data taken in 1997 and beyond is well underway. We have estimated the full volume of data that will be available for studies of a number of channels with the full pre-upgrade luminosity by extrapolation from event yields in 1996. We have also estimated the yields for a total luminosity of $600\ \mathrm{pb}^{-1}$, which is the luminosity expected to be delivered by HERA in the minimum proposed four years of running after the upgrade. Table 1 shows these estimates.

The extrapolation factors for the numbers of events in the table are based on the ratio of luminosities delivered by HERA.[3] Thus, corrections for the efficiency with which H1 takes data that is usable for analysis are implicitly made under the assumption that this efficiency will remain unchanged after the upgrade. Trigger and reconstruction efficiencies are assumed to be comparable to those for the 1996 run, such that the figures for the upgraded HERA assume the existence of the FTT. It should be noted that with the present data rates, the H1 trigger and data acquisition system is already unable to take data throughout the full available phase space for many processes. Random downscaling of triggers is often required and it is often necessary to apply

[3] For the estimated yields in the years 1997-2000, it is assumed that HERA will deliver $35\ \mathrm{pb}^{-1}$ in the e^+p run currently in progress.

PROCESS	EVENTS FROM 1996 DATA ($13\ \mathrm{pb}^{-1}$ DELIVERED)	ESTIMATED EVENTS $1997-2000$ ($92\ \mathrm{pb}^{-1}$ DELIVERED)	ESTIMATED EVENTS POST-UPGRADE WITH FTT ($600\ \mathrm{pb}^{-1}$ DELIVERED)
D^* in DIS ($Q^2 > 2\ \mathrm{GeV}^2$)	583	4100	27000
D^* in DIS FROM b DECAY	(9)	(60)	(420)
D^* in diffractive DIS ($Q^2 > 2\ \mathrm{GeV}^2$)	11	80	510
D^* in γp	788	5500	36000
D^* in γp FROM b DECAY	(13)	(90)	(600)
Elastic $\rho^0 \to \pi^+\pi^-$ ($Q^2 > 30\ \mathrm{GeV}^2$)	16	110	740
Quasi-elastic $J/\psi \to \mu^+\mu^-$ ($Q^2 > 2\ \mathrm{GeV}^2$)	156	1100	7200
Quasi-elastic $J/\psi \to e^+e^-$ ($Q^2 > 2\ \mathrm{GeV}^2$)	74	520	3400

Table 1: Event yields for processes of interest to the FTT, assuming selection criteria as applied in the most recent publications [2, 12, 15, 16]. The second column shows the number of events on which H1 publications on 1996 data are based. The third column shows the expected number of events that will be available before the major shutdown, obtained by extrapolation of the figures from the 1996 publications. The final column shows the number of events expected from a sample of $600\ \mathrm{pb}^{-1}$, also obtained by extrapolation of the 1996 figures. The numbers in parentheses are estimated by assuming that $1.6\ \%$ of all D^* candidates arise from b decays [2].

rather tight selection criteria in the latter stages of the trigger. For example, D^* events in photoproduction are presently discarded if the D^* transverse momentum is calculated at the level 4 stage of the trigger to be less than $1.9\ \mathrm{GeV}$. This number should be compared with the analysis cut used in 1996 data of $1.5\ \mathrm{GeV}$. The data volumes obtained in 1997-2000 therefore do not quite scale with the luminosity relative to 1996 data for many processes as assumed in the table. The numbers quoted for the pre-upgrade yields should be thought of as upper limits.

The predicted totals of 4100 D^* events in DIS and 5500 in photoproduction available for analysis before the upgrade represent a considerable improvement on the statistics used in the published analysis. With these data volumes, it will be possible to improve the statistical precision on the gluon distribution of the proton (figure 1 of the original proposal) by a factor of around 2.5. However, this still only scratches the surface of the detailed heavy flavour physics exploration possible at HERA. Additional statistics would allow the measurement of the $x_g g(x_g)$ distribution as a function both of x_g and of the factorisation scale μ^2, which would provide a much more sensitive test of the underlying QCD dynamics and of resummation techniques.

The predicted yields of J/ψ events after the upgrade would allow high precision measurements in both DIS and photoproduction of the elastic cross section differentially in both the Mandelstam s and t variables for the $\gamma^* p$ system. The elastic J/ψ cross section is something of a special case in diffractive physics at HERA, exhibiting a strong 'hard pomeron'-type s dependence even at $Q^2 = 0$. Large data sets will be required to answer conclusively the question of whether the centre of mass energy dependence varies with Q^2 in the manner predicted in models based on the exchange of gluon pairs [18]. Any change in the s dependence as t varies would imply the shrinkage of the diffractive peak associated with the slope α' of the pomeron trajectory. The presence or absence of this shrinkage and its dependence on Q^2 is a very important question to the understanding of hard diffraction [19].

For the remaining example channels in table 1, it is clear that the statistics will still be rather poor when the upgrade takes place. The yields of detectable D^* mesons from beauty decays and from diffractive processes are such that measurements with sufficient precision to seriously test models will not be possible until well after the upgrade. As discussed in section 3.1 of the original proposal, vector meson production cross sections are very heavily suppressed with increasing Q^2. Only with the use of the FTT after the upgrade it will be possible to make precision measurements of the elastic ρ cross section in the region $30 \lesssim Q^2 \lesssim 100\ \mathrm{GeV}^2$. This high Q^2 region is the most sensitive to the QCD dynamics of diffraction.

3.2 Trigger Efficiencies With and Without the FTT

Table 2 of the original proposal showed estimated trigger efficiencies with and without the FTT after the upgrade. It is reproduced here in a slightly updated form as table 2. As stated in the original document, the numbers quoted are rather tentative, as there are many unpredictable factors that cannot yet be taken into account. For example, the L1 trigger rates depend strongly on the beam conditions and on the trigger combinations actually used. These will have to be optimised after the upgrade, but the discrimination at L2 and L3 available from the use of the FTT is likely to allow L1 rates to remain rather high.

Full details of the assumptions made in producing the table are given in appendix A. Note that for some channels, other means of triggering are possible in addition to those based on tracks. The triggering efficiency for $W \to \mu\nu$ based on a relatively unbiased muon trigger would be 3% after trigger downscaling without the FTT due to the high level 1 rate of such a trigger. The overall H1 trigger efficiency for this channel would be larger if, for example, a missing p_t trigger were used in conjunction with the muon trigger. However, the threshold of the missing p_t trigger would restrict the kinematic region available for the measurement considerably to about 20-30% depending on the actual cut. For channels such as this (and also for heavy vector meson and Z^0 decays to lepton pairs), the FTT would complement other methods of triggering.

	trigger rates with FTT [Hz]			visible cross section	trigger efficiency [%]	
Process	**L1**	**L2**	**L3**	σ_{vis} [pb]	with FTT	without
D^* decay (DIS)	160 - 500	30	5	150	70	1
D^* decay (e-tagged γ p)	120 - 500	25	4	100	60	1
$\rho \to \pi^+\pi^-$ (DIS)	40	2.5	1	5000	80	2
J/$\Psi \to$ ee,$\mu\mu$	50	20	1-3	1000	12-60	1-3
$\upsilon \to$ ee, $\mu\mu$	50	5	0.5-2	1.5	12-60	1-3
W $\to \mu\nu$	20	1	0.3	0.1	70	3

Table 2: (slightly modified from original proposal). Estimate of trigger rates and their reduction at the three different levels with and without the help of the Fast Track Trigger. The total visible cross section is also shown. The rates are tentative and scaled to the expected peak luminosity of $70\ \mu\text{b}^{-1}\text{s}^{-1}$. The L1 triggers used and L2 and L3 conditions applied with the FTT are described in appendix A. The trigger rates for vector mesons differ for elastic and inelastic production because of the varying effectiveness of the track multiplicity requirement. Note that D^* mesons produced in b decays or in the diffractive channel are indistinguishable from the bulk of D^* candidates at the trigger level and are thus subject to the same efficiencies with and without the FTT as those shown in the table.

3.3 Gain as a Function of Kinematic Phase Space

It is not possible at this stage to anticipate in detail the triggering strategy after the upgrade in the absence of a FTT. However, it is possible to make some more general statements based on the current procedures.

Where the scattered electron is identified in the liquid argon calorimeter ($Q^2 \gtrsim 100\ \text{GeV}^2$), H1 currently accepts all triggered events. This is also likely to be the case after the upgrade. In the $Q^2 = 0$ photoproduction regime, events are universally discarded unless special signatures for interesting events are identified by the trigger.

At intermediate Q^2, where the electron is scattered into the backward spaghetti (SPACAL) calorimeter, there is already considerable event reduction unless special signatures are identified. A system of random downscaling is applied at the level 1 trigger stage in order to restrict the input rate to the level 4 filter farm to a manageable

level. The downscaling factor varies with the luminosity and with the radial position of the electron cluster, and is largest at low Q^2. It is possible that after the upgrade, minimum bias SPACAL triggers will be completely disabled. The best scenario is that the total SPACAL L1 output rate will be maintained at a similar level to the present. The HERA upgrade is expected to yield a factor of order 5 increase in instantaneous luminosity. As a working hypothesis, we therefore assume that the prescale factors applied to SPACAL triggers will also be increased by this factor.

On the basis of these assumptions, table 3 summarises the expected losses of efficiency due to random downscaling in the absence of a FTT for average luminosities before and after the upgrade. Note that the prescales at peak luminosity (as considered in table 2) are at least a factor of two larger than those shown here. The figures apply to any process that cannot be identified using the early stages of the trigger. Thus, certain types of easily identified signature, such as high $p_{_t}$ jets or muon pairs, would not be subject to these losses in efficiency. More complex signatures of the type that the FTT is required to identify, such as D^* candidates, require more information and complex computing operations. This is presently realised at the level 4 stage of the trigger. Events such as those containing D^* or ρ candidates will therefore be subject to the downscaling and resulting efficiencies as shown in table 3 along with the bulk of events which contain no unusual signatures.

Q^2	PRESENT PRESCALE	PRESCALE AFTER UPGRADE	RESULTING EFFICIENCY (%)
0	∞	∞	0
5	5	25	4
40	2	10	10
150	1	1	100

Table 3: Expected level 1 prescales at average luminosities before and after the upgrade for events triggered on the basis of an identified electron and minimal track requirements, where no further interesting signatures are recognised at the trigger level. The figures for after the upgrade assume that there is no FTT.

3.4 Systematic Limitations

As explained in section 3.2, statistical limitations are likely to remain severe for many of the processes of interest until well after the upgrade. Nonetheless, it will clearly be crucial to obtain the triggering efficiency for all relevant processes with high accuracy in order to avoid large systematic uncertainties from the use of the FTT. One important aspect in this is that the triggering efficiency itself will be very high for most processes of interest. Provided this is the case, small uncertainties in the efficiency will not lead to large uncertainties when propagated to final measurements. The trigger efficiency will be obtained by a combination of detailed simulation and direct extraction from data.

The operation of the FTT will, for the most part, be digital, such that all features of its operation, including variations in FPGA loads, can be simulated with full accuracy. The crucial aspect will be to correctly simulate the hit finding efficiency of the $Q-t$ analysis in the level 1 board. Considerable effort will clearly have to be invested in this aspect of the problem. The aim is to simulate FTT track-finding efficiencies to an accuracy at the percent level, which should be considerably better than that required for the majority of applications.

The FTT efficiency can also be determined directly from the data. This will be essential in order to cross-check the simulated efficiency of the $Q-t$ algorithm. Track segment and full track efficiencies could be determined by taking samples of tracks reconstructed in the CJC and measuring the efficiency with which the FTT also found those tracks as a function of the track $p_{_t}$, θ and ϕ. It may also be possible to go one stage further and obtain full FTT efficiencies for a given physics channel such as a D^* search. This could be done by studying samples of D^* candidates collected with a highly downscaled minimally biased SPACAL trigger, though statistics may become a problem in this latter case.

4 FTT Performance

Considerable progress has been made in the simulation of the intended FTT algorithms since the original proposal was submitted. Here we provide an update on the simulated performance of the trigger and present a detailed analysis of the robustness of the device.

4.1 Use of the Vertex Trigger

It is intended that information from the MWPC based level 1 z-vertex trigger will be available to the FTT at the track segment finding stage. This gives coarse information on the position of the event vertex in the direction along the beamline (see figure 3a). It has now been possible to include the z-vertex trigger information in the simulation. This leads to a significantly better resolution in θ for tracks. As a result, the expected performance of the FTT improves considerably compared with the previous simulation used for the original proposal, where no vertex information was included. In the following sections, the performance of the FTT with the updated simulation is discussed.

4.2 Track Resolution

A poor track resolution results in poor signal to background ratios for level 2 FTT cuts in e.g. p_t. It also implies that level 3 cuts on invariant masses have to be rather loose, decreasing the selectivity of the FTT. The track parameter resolution is therefore a key-point for the design of the FTT. Figure 2 (a) shows the simulated precision of the measurement of $1/p_t$ for all tracks reconstructed in D* candidate events in the year 1997. Figure 2 (b) shows the resolution on ϕ. Both figures show the resolution of the FTT with respect to the full off-line reconstruction. The resolution in p_t is approximately $\sigma_{p_t} = 4\% \frac{1}{p_t^2}$. That in ϕ is approximately 5 mrad.

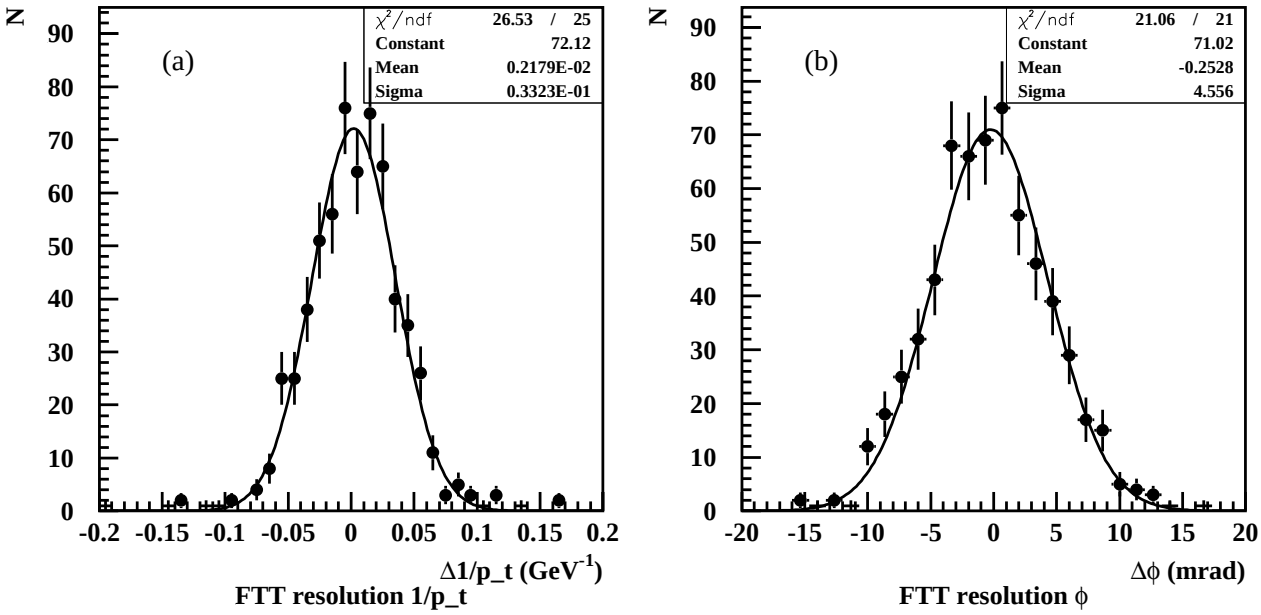

Figure 2: Track resolution of the simulated FTT algorithm in (a) $1/p_t$ and (b) ϕ relative to the full off-line CJC reconstruction. The tracks studied are taken from a sample of $D^* \to K\pi\pi_{\rm slow}$ candidates in 1997 data. Gaussian fits are shown to both distributions.

The polar angle resolution of tracks depends on two parameters, the z-position of the ep interaction vertex and

the single hit z-resolution of the CJC. The primary vertex position is determined by the peak position of the z-vertex histogram reconstructed from tracks measured by the MWPCs. The z-vertex resolution for D* events is shown in figure 3 (a). The resolution relative to the full off-line reconstruction is about 2.3 cm, which should be compared with the Gaussian width of the actual z-vertex distribution of approximately $30\,\mathrm{cm}$. The single hit z-resolution of the CJC, as determined by charge division, is a function of the total charge collected by single wires. The dependence is shown in figure 3 (b). Typical amplitudes of the collected charge are 500-1000 units resulting in a single hit resolution of 5-8 cm in the z-direction. Based on these parameters, the polar angle resolution of tracks in D* events, shown in figure 4, is approximately 50 mrad.

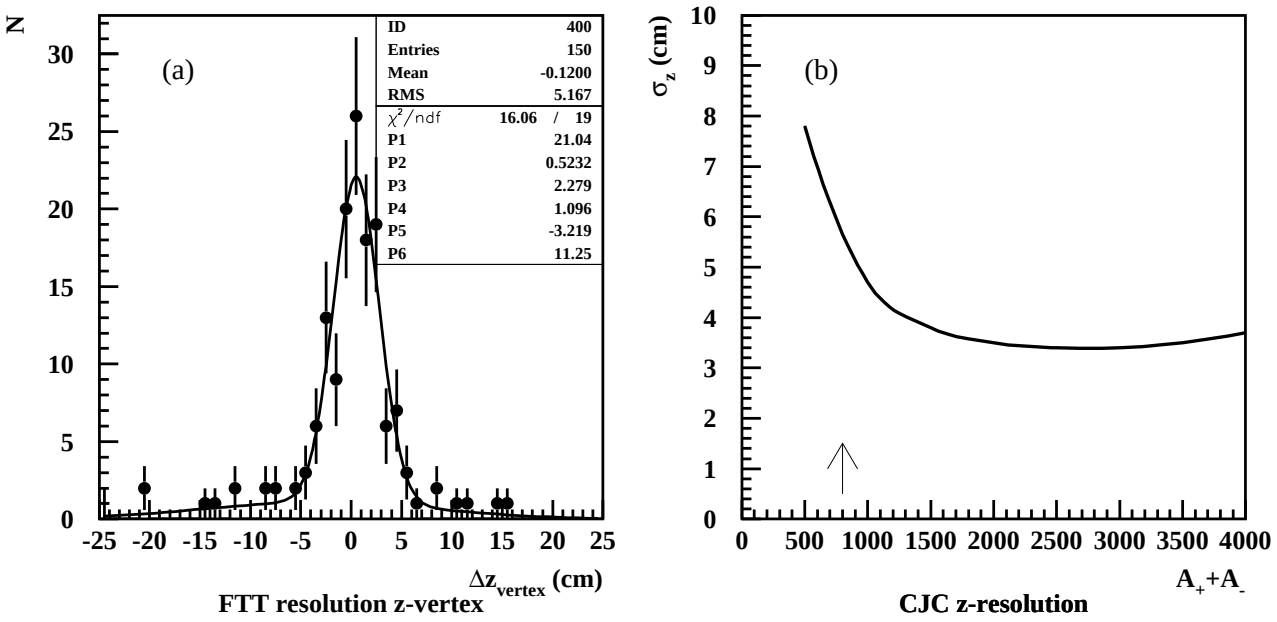

Figure 3: (a) Resolution of the MWPC based z-vertex trigger with respect to the full off-line reconstruction, including information from drift chambers designed to measure the z coordinate. The data used are a sample of $D^* \to K\pi\pi_{\mathrm{slow}}$ candidates in 1997 data. The fit shown is to a sum of two Gaussian distributions. (b) Dependence of the single hit z-resolution of the CJC, obtained by charge division, on the integrated charge collected at both ends of a wire (arbitrary units) [20].

4.3 D^* Finding Efficiency and Trigger Rates

In order to maintain high selectivity and thus keep trigger rates as low as possible, it is important that the resolution of the FTT should be as good as possible on the invariant mass sums that form the basis of the L3 decision. Triggering on the $D^* \to D^0\pi_{\mathrm{slow}} \to K\pi\pi_{\mathrm{slow}}$ channel will be realised through cuts on the reconstructed D^0 mass and the reconstructed mass difference $\Delta M = M(D^*) - M(D^0)$. In figure 5, the simulated FTT resolution on these parameters is illustrated. A sample of D^* candidates from 1997 data is used, subject to the selection criteria with the full H1 reconstruction $|M(K\pi) - M(D^0)| < 80\ \mathrm{MeV}$ and $M(K\pi\pi_{\mathrm{slow}}) - M(K\pi) < 150\ \mathrm{MeV}$. For this sample of events, the figure shows the distribution in the reconstructed D^0 mass (a) and the reconstructed mass difference ΔM (b). The main effect of the improved vertex treatment is that the D^0 mass is much better resolved (Gaussian width of approximately $78\ \mathrm{MeV}$, which should be compared with a resolution of $61\ \mathrm{MeV}$ using all available off-line analysis tools with the full CJC information).

The inclusion of z-vertex trigger information improves efficiencies and reduces background rates for a given set of selection criteria in a given channel. The efficiency and trigger rate predictions are shown in figure 6a. For

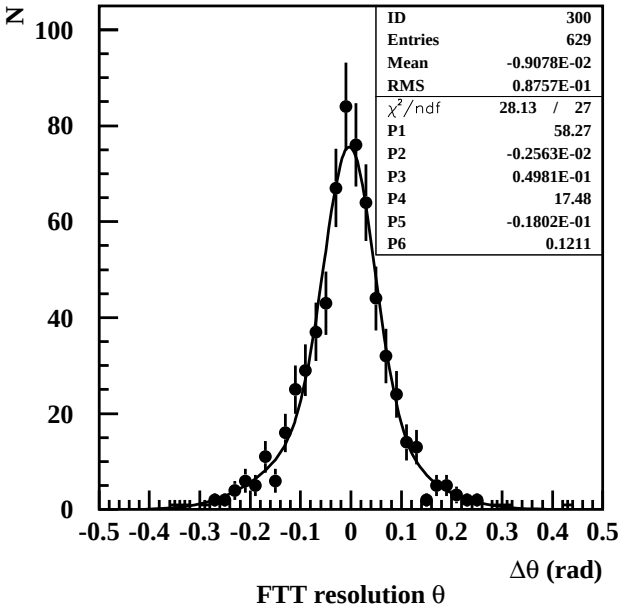

Figure 4: Resolution of the simulated FTT algorithm in θ with respect to the full off-line reconstruction. The FTT z-vertex measurement is taken from the MWPC z-vertex trigger and the single-hit z-resolution from charge division. The off-line reconstruction also uses information from drift chambers designed to measure the z coordinate. The fit shown is to a sum of two Gaussian distributions.

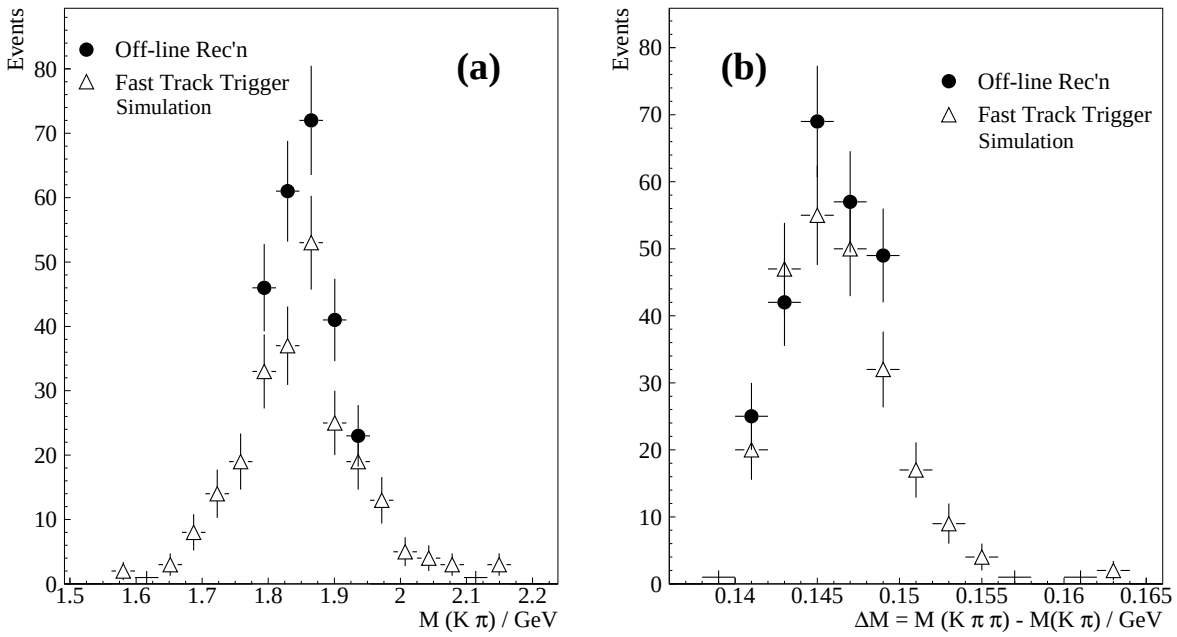

Figure 5: Illustration of the expected resolution on (a) $M(D^0)$ and (b) ΔM with the proposed trigger. The solid points show the distribution for a sample of D^* candidates from DIS events collected by H1 in 1997, reconstructed with the best available off-line analysis tools and subjected to the selection criteria $|M(K\pi) - M(D^0)| < 80$ MeV and $M(K\pi\pi_{\rm slow}) - M(K\pi) < 150$ MeV. The open triangles show the distributions for the same sample of events reconstructed using the simulation of the proposed FTT.

comparison, figure 6b, which is a copy of figure 4 of the original proposal, shows the efficiencies and expected trigger rates in the case where no information on the vertex is available. With the z-vertex information added, a selection at the level 3 stage with $|M(K\pi) - M(D^0)| < 200$ MeV and $\Delta M < 155$ MeV would give an efficiency of around 80%, whilst restricting overall trigger rates to less than 5 Hz at peak luminosity after the upgrade. Comparable improvements are expected in the performance of the proposed FTT for all other channels.

4.4 Robustness

The details of the running conditions for the H1 drift chambers after the upgrade cannot accurately be predicted at this stage, due to the very large number of parameters that affect them. The most pessimistic estimates suggest that there may be activity on as many as 10% of CJC wires at a given bunch crossing. Currently the rate of background hits in the CJC under normal running conditions is well below 1%. The FTT must be able to cope with the increased instantaneous chamber occupancy and must also be able to run with high efficiency if bad running conditions enforce a reduction in the gain of the drift chambers.

We have used the simulation of the FTT to investigate the sensitivity of the proposed device to a number of different types of degradation in the running conditions. The following sections show the resulting effects on D^* finding, which will be among the most complex final state signatures that the FTT is required to identify, and on J/ψ finding.

4.4.1 Failure of the MWPCs

It is sometimes the case that there are trips in the forward or central tracker MWPCs, such that z-vertex trigger information reduces in quality or ceases to be available.[4] It is clear from a comparison of figures 6a and 6b that the FTT can continue to provide triggers with reasonable efficiency at times when the CJC is operational but the z-vertex trigger is not. The loss of FTT triggering efficiency under these circumstances depends on the channel and choice of trigger cuts, but for the D^* case, the efficiency would drop from around 80% to around 60%.

4.4.2 Reduced Single Hit Efficiency

In the simulations, the single hit efficiency is assumed to be 95% by default. This is similar to the values achieved with the present DC$r\phi$ track trigger using comparable thresholds to those likely to be used for the FTT. The effect on track reconstruction efficiencies of degrading the single hit efficiency can be seen in figure 7. Due to the high redundancy of the proposed FTT (a coincidence of only two of the possible four track segments is required to form a track, whereas the mean number of segments linked for tracks from D^* decays is around 3.5 at 95% single hit efficiency), a considerable reduction in single hit efficiency can be tolerated before the overall track finding efficiency degrades to the point where the FTT effectively becomes inoperational. For the most central tracks (pseudorapidity $\eta \sim 0$), the efficiency losses are less than those for tracks at the extremes of the CJC acceptance ($|\eta| \sim 1.5$). This is because the tracks at the extremes of the FTT acceptance often do not reach CJC2 and thus do not typically pass through all four groups of wires used by the FTT.

Figure 8 shows the effects on the D^* reconstruction efficiency of reducing the single hit efficiency of the FTT. The efficiencies fall by only around 10% when the single hit efficiency is reduced from 95% to 90%. There is no reason whatsoever to suppose that the single hit efficiency could be as low as 90% in normal operation,

[4] The proposed upgrade of the central inner proportional chambers (CIP) is intended to improve the robustness of the z-vertex trigger.

(a) z-vertex trigger information included

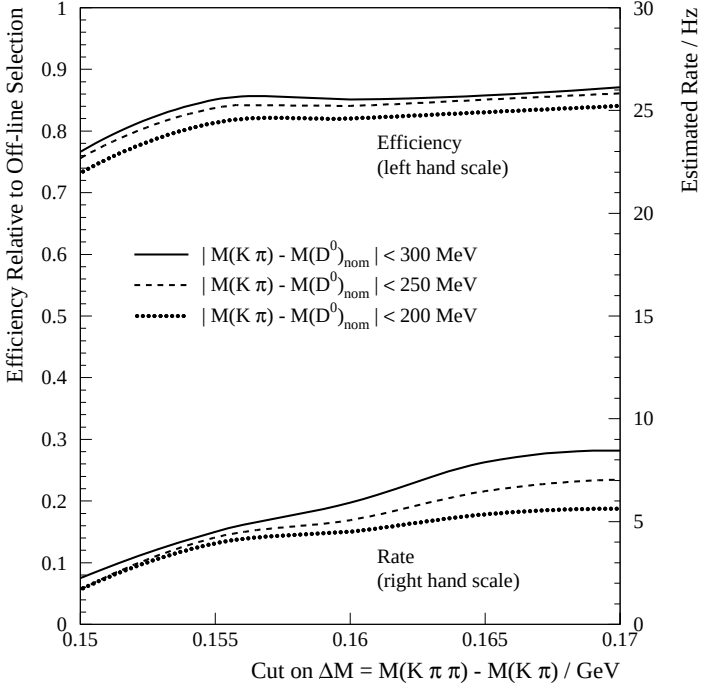

(b) z-vertex trigger information not included

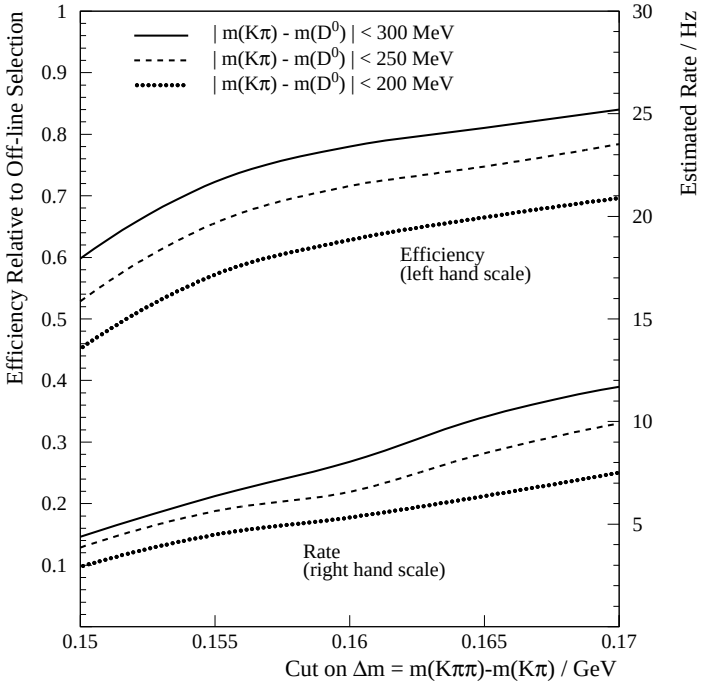

Figure 6: Estimated efficiencies and trigger rates for D^* mesons in DIS using the proposed trigger for various choices of cut on the reconstructed D^0 mass and ΔM. In (a) the information from the MWPC z-vertex trigger is used. In (b), which corresponds to figure 4 of [1] , the z-vertex trigger information is not used. The efficiencies are relative to the off-line event selection used in the most recent H1 publication [2] and are calculated using a sample of DIS events collected in 1997. The expected rates are estimated using a sample of events collected using a SPACAL electron trigger and are extrapolated to the peak luminosity of $7 \times 10^{31}\ \mathrm{cm}^{-2}\mathrm{s}^{-1}$ that the upgraded HERA is expected to deliver.

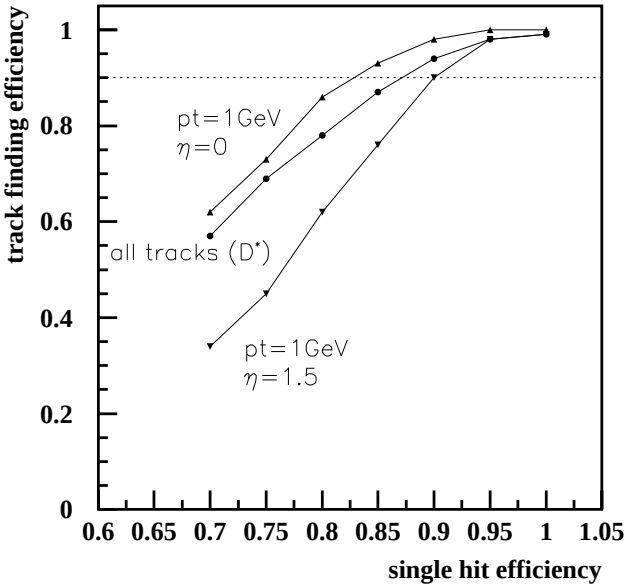

Figure 7: FTT track reconstruction efficiencies as a function of the single hit efficiency. Results are shown for tracks with $p_{\mathrm{t}} = 1\ \mathrm{GeV}$ in the centre of the CJC acceptance ($\eta = 1$) and at its extreme limit ($\eta = 1.5$) and for an average over all tracks arising from $D^* \to K\pi\pi_{\mathrm{slow}}$ decay candidates in 1997 data.

provided reasonable thresholds are assigned in the $Q - t$ algorithm. That the efficiencies remain so high when the single hit efficiency is degraded in this manner illustrates the overall robustness of the proposed device. Even when the single hit efficiency is degraded to 80% in the simulation, the D^* finding efficiencies remain in the region of 45%. Such a situation is totally unrealistic, but even in this scenario, the FTT would still be an effective trigger for D^* finding. We conclude that poor single hit efficiencies are not likely to be a problem for the FTT.

4.4.3 Worsened z-Resolution

In the simulations performed thus far, the z coordinates of hits are assumed to be obtained by charge division with a resolution of $6\ \mathrm{cm}$ (compare figure 3b). The charge division resolution is a strong function of the gain of the CJC, so the FTT may have to cope with lower single hit z-resolution if it becomes necessary to reduce the gain. We have investigated a situation in which the z-resolution is worsened to $10\ \mathrm{cm}$. As can be seen from figure 3, this is a somewhat extreme case. The effects on D^* triggering efficiency are shown in figure 8. Even in this scenario, the efficiencies fall by only around 5%, a smaller reduction that the gain achieved with improved z-vertex information (figure 6).

The effects of degrading the single hit efficiency and single hit z-resolution have also been studied for J/ψ data. In figure 9, invariant mass distributions are shown in both the $\mu^+\mu^-$ and e^+e^- channels from elastic J/ψ candidates from 1997 data. The distributions obtained from the full reconstruction are compared with those from the tracks reconstructed by the FTT. Figures 9a and 9b show the results using the FTT with the expected CJC operating conditions for normal running. Approximately 97% of the off-line muon candidates in each channel are successfully identified by the FTT algorithm. Figures 9c and 9d show the effects of reducing the single hit efficiency to 90% and the single hit z-resolution to $8\ \mathrm{cm}$. The efficiencies in each channel are reduced to approximately 89%, due to the lower single hit efficiency. The degradation in single hit z-resolution results in only a small deterioration in the J/ψ mass resolution. This will not present any problems for the FTT triggering of J/ψ events, as backgrounds are relatively small in this region. A mass window of $0.5\ \mathrm{GeV}$ around the nominal J/ψ mass is currently proposed (see table 2 and appendix A), which leaves a very wide safety margin for poor running conditions.

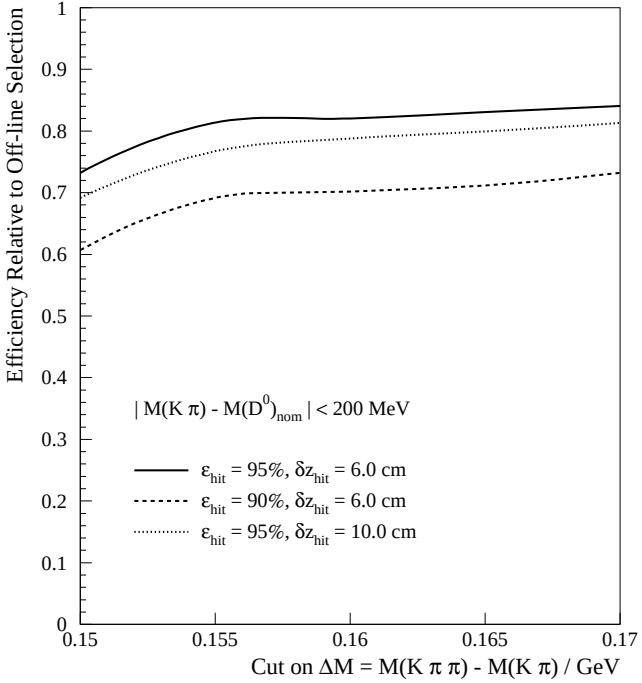

Figure 8: Estimated efficiencies and trigger rates for D^* mesons in DIS using the proposed trigger for various choices of cut on the reconstructed D^0 mass and ΔM with different single hit efficiencies ($\varepsilon_{\rm hit}$) and single hit z-resolutions ($\delta z_{\rm hit}$). The efficiencies are relative to the off-line event selection used in the most recent H1 publication [2] and are calculated using a sample of DIS events collected in 1997.

4.5 Increased Instantaneous Chamber Occupancy

As a final test, we have investigated the sensitivity of the trigger to increased instantaneous numbers of signals in the CJC. This could arise due to severe problems with noise or with synchrotron radiation or beam-gas backgrounds. Overlap of information from different ep collisions is already known not to be a severe problem. In the tests, we added random background CJC hits to existing H1 events. The number of added hits was randomly distributed between 100 and 500, corresponding to activity on between 4% and 20% of CJC wires. Only those events for which at least three additional tracks were found by the full off-line reconstruction as a result of the added noise hits were retained for analysis.

The presence of the extra hits slightly improves the D^* finding efficiency, due to random coincidences with genuine tracks arising from D^* decays. This is a slightly unrealistic situation, as the potentially degrading effects on the $Q-t$ algorithm of overlapping hits is not yet included. Work on the evaluation of this effect is in progress.

In section 3.4 of [1] and in section 4 above, a sample of events collected in 1997 using an inclusive SPACAL level 1 trigger, with the subsequent trigger levels disabled, was used to estimate the overall trigger rates of the FTT when extrapolated to the post-upgrade peak luminosity. This sample represents a good approximation to the overall event sample with which the FTT will be confronted in the intermediate Q^2 region. We have introduced additional noise hits to these data in the manner described above, in order to test the sensitivity of the background rates to increased chamber occupancy. The results are shown in figure 10 as function of the ΔM cut and demonstrate that the effect of additional background can be strongly suppressed by using tight selection criteria. It is clear that considerable increases in background hits can be tolerated without the D^* finding algorithm yielding excessive numbers of background events.

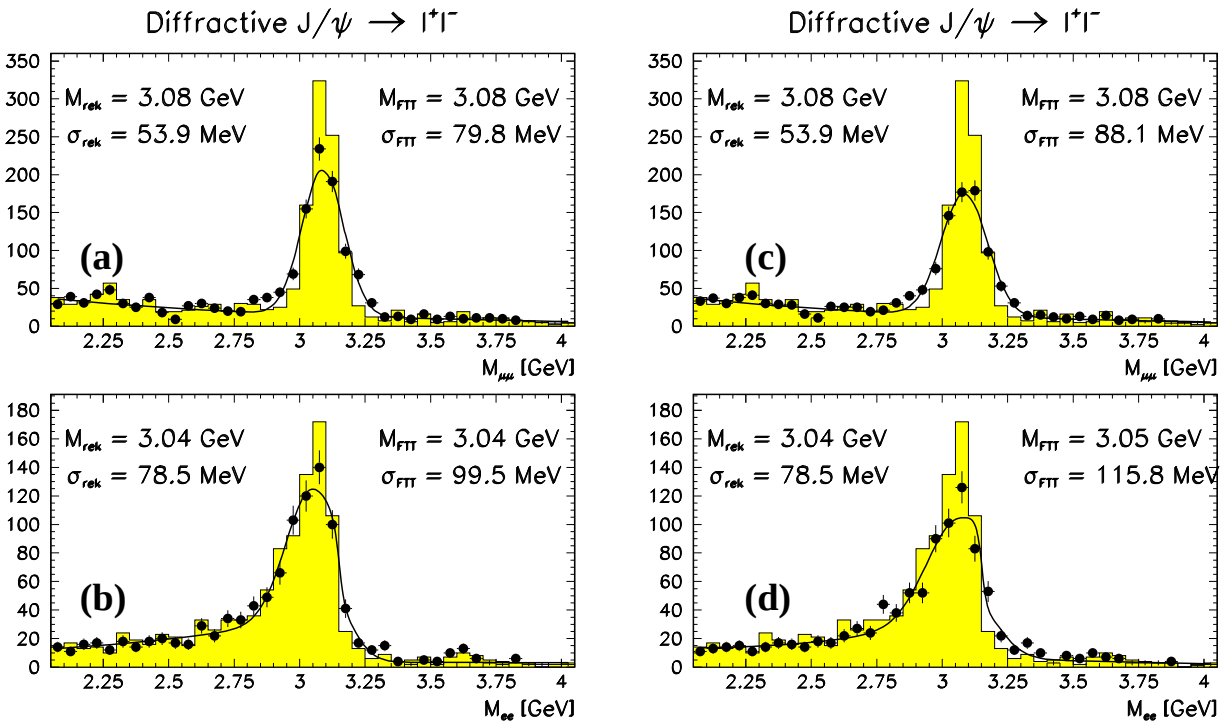

Figure 9: Distributions in the reconstructed dilepton invariant mass for a sample taken from 1997 elastic J/ψ data. (a) and (c) show the distributions of $\mu^+\mu^-$ invariant masses. (b) and (d) show the e^+e^- invariant masses. For all plots, the histograms show the distributions as reconstructed with the full readout information and the best available off-line tools. The solid data points show the distributions as reconstructed from tracks produced by the FTT simulation. In (a) and (b) the essential parameters of the FTT operation assume their default values (single hit efficiency of 95% and single hit z-resolution of 6 cm. In (c) and (d) the single hit efficiency is degraded to 90% and the single hit z-resolution to 8 cm.

5 Project Specification and Realisation

5.1 Level 1 Trigger Signal

The possibility that the FTT could provide information to the level 1 trigger is currently being investigated. This could be implemented with the addition of one further FPGA per level 1 crate, which would process the coarse track segment information. It is not yet clear whether it will be possible to generate a coarse $1/p_t - \phi$ histogram of the track segments and perform a simple track linking algorithm. If this is possible, the level 1 information could be based on the multiplicity of tracks and their transverse momenta in much the same way as the planned level 2 algorithm. If it is not possible to form full tracks at level 1, track segment multiplicities and topologies could be used as the basis for a decision.

The cost of including the trigger functionality at level 1 would be at the level of 70kDM, corresponding essentially to the cost of the FPGAs. If a level 1 trigger were implemented, the existing DC$r\phi$ trigger could be replaced completely.

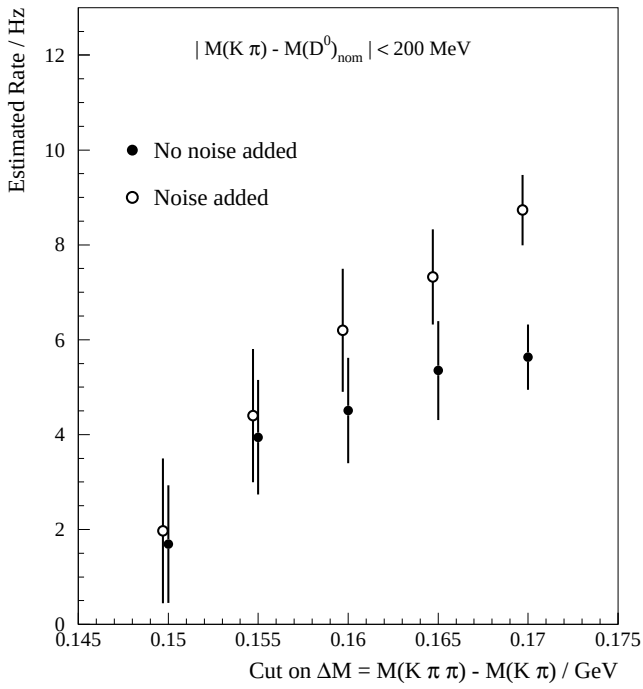

Figure 10: Estimated background rates for the FTT D^* SPACAL trigger at the expected peak post-upgrade luminosities. The rates are shown as a function of the L3 ΔM cut for a D^0 mass cut of $|M(D^0) - M(K\pi)| < 200\ \mathrm{MeV}$, with and without additional noise added to the CJC (see text for details).

5.2 Hardware Implementation and Time Considerations

It is intended that all tasks required of the FTT, up to and including a level 3 trigger decision, should be performed within about $100\ \mu\mathrm{s}$ of the ep interaction. The information that will be provided to the level 1 (2.3 μs), level 2 (25 μs) and level 3 stages of the trigger is as illustrated in figure 7 of [1]. The time limits for the first two trigger levels impose strict requirements on the FTT algorithms. The problem of pattern recognition is accomplished using devices such as Content Addressable Memories (CAMs) which are capable of performing complex logical operations at high speed, performing search tasks in single cycles of typically $\sim 10\ \mathrm{ns}$. A similar time scale applies to Digital Signal Processors (DSPs) which are used after the track linking procedure for the optimisation of track parameters. A precise statement on the necessary computation time would require the algorithms and their realisation in hardware to be completely defined. At this stage, only estimates can be made on the basis of the current plans.

5.2.1 Level 1 Timing

The time available for logical processing to produce a L1 trigger decision is significantly reduced by the maximum CJC chamber drift time. Pipelining of information is forseen, such that valid combinations of hits based on a pivot layer technique step through shift registers and are compared against lists of acceptable hit patterns using CAMs, only the drift time of the combination being changed at each cycle. High speed is achieved with a highly parallel algorithm with a simultaneous matching procedure using a "CAM farm". Valid track segments can then be found within a few cycles. The estimated timing of the different L1 tasks is listed in table 5.

Process	time [μs]
drift time of most distant hits	1.0
$Q - t$ analysis	0.3
filling of shift registers	0.1
track segment finding	0.2
collecting track segments	0.2
L1 trigger processing	0.2
total	2.0

Table 4: Timing specifications at trigger level 1. Note that the track segment finding begins before all drift times are available, such that several bunch crossings are processed in parallel. The figure of 0.2 μs quoted for track segment finding thus represents the actual delay incurred, rather than the full time necessary to process a single event.

5.2.2 Level 2 Timing

At L2, the most time consuming process is the optimisation of the track parameters in the r-ϕ and r-z planes after the track segment linking. First studies with C6201 (fixed point DSP) and C6701 (floating point DSP) running on non-optimised reconstruction code indicate that this task can be performed within 8 μs. The timing of L2 is detailed in table 5 and shows a safety margin of 4 μs. Replacing the sliding window technique by a simple one step matching procedure would accelerate the L2 linking by a further 4.5 μs at the expense of a small degradation in the track separation power.

Process	time [μs]
read data from track segment finder	1
distribute data to all L2PUs and load CAMs	2
dynamic load balancing (counters)	1
Search including using 4 sliding windows	6
optimise track parameter values (DSP)	8
distribute track parameters and calculate sums	2
communicate result to L3	1
total	$\leq$21

Table 5: Estimated timing specifications for the L2PUs. Note that several tasks can be interleaved.

5.2.3 Level 3 Timing

At L3, the mass reconstruction will be performed using commercial processors. Tests with a Pentium II processor have shown that a single track combination to calculate an invariant mass will take about 50 ns at a clock frequency of 500 MHz. Within 100 μs about 2000 mass combinations can be analysed on a single processor. Less than 30 tracks are reconstructed by the simulated FTT algorithm for over 96% of 1997 D^* candidates, such that a single processor would be more than sufficient to make D^0 and subsequent D^* searches. By adding more processors to the L3 trigger level, a latency well below 100 μs can be achieved, whilst searching for a wide variety of signatures. It should be pointed out that in contrast to the L1 and L2 time limits, the 100 μs L3 limit is 'self-imposed' on the FTT. A slight increase in the L3 processing time would result only in a small delay in the level 3 reject signal and a commensurate small increase in deadtime.

5.3 Responsibilities and Manpower

The hardware implementation of the FTT is divided into three parts. The front-end and the custom boards for L1 are being developed and built by UK groups. The custom boards at L2 are being developed by the SCS company in Zürich in collaboration with ETH Zürich. The L3 processor farm will be constructed by the Dortmund group. An overview of the hardware responsibilities and allocated manpower is given in table 6. The implementation of the software algorithms in the programmable hardware requires further manpower. These allocations are shown in table 7.

Hardware Tasks	Effort in SY	Responsibilities
Analogue daughter cards	1	RAL/Manchester
L1 Front-End Module with track segment finder	3	RAL
L1 crate controller	2	Manchester/Birmingham
L1 trigger card*	1	QMW/Birmingham/DESY
L2PU Track Linker boards	2	Zürich/SCS
L2/L3 Trigger card	1	SCS/Dortmund
L3 processor farm	1	Dortmund

Table 6: Manpower allocations for FTT hardware construction tasks. * Note that the L1 trigger card is a design option which will allow to generate L1 Keep signals and would replace the existing DC$r\phi$ trigger.

Software Tasks	persons	Responsibilities
Setup $Q - t$ algorithm	1	RAL
Programming of L1 track segment finding	2	DESY/Zurich/Birmingham
Programming of L2PU boards	2.5	Zurich/ETH/Dortmund
L3 processor farm	1	Dortmund

Table 7: Manpower allocations for the design and implementation of software algorithms in the FTT system.

5.4 Financing

All anticipated costs of the FTT project are detailed in table 8. A complete financing scheme now exists. The UK institutes collaborating in H1 (Birmingham, Lancaster, Liverpool, Manchester, QMW and RAL) are in the process of submitting a proposal to the UK PPESP, requesting approximately 770kDM for the L1 construction. DESY is encouraged to support the project at the level of about 250kDM. 250kDM have been set aside from BMBF funds which hopefully can be expanded to a total of 500kDM. An additional equivalent of about 500kDM in skilled manpower will be provided by ETH Zürich and Dortmund to work with the SCS company on the level 2 system. Assuming all requested funds are released, the total funding will amount to 2020kDM, leaving 70kDM free for extra contingency.

References

[1] H1 collaboration, *A Fast Track Trigger with High Resolution for H1*, Proposal submitted to the Physics Research Committee, PRC 99/06.

[2] H1 Collaboration, C. Adloff et al., Nucl. Phys. **B545** (1999) 21.

[3] ZEUS Collaboration, J. Breitweg et al., DESY **99-101**, submitted to Eur. Phys. J.

Item	Quantity	cost [kDM]
Analogue daughter cards	150	100
L1 Front-End Module	30	470
L1 Crate Controller	2	35
L1 trigger card*	2	35
Crate	2	70
Cabling	various	40
Workstation and Interface	1	20
L2PU hardware	4	100
L2PU external labour (SCS)	2SY	500
L2PU supplied labour	2SY	*500
L2L3 trigger card	1	20
L3 processor farm	1	60
total		1950

Table 8: Full costing of the FTT project, including external labour and VAT. * Note that the L1 trigger card is a design option which will allow L1 Keep signals to be sent to the central trigger. The FTT would then completely replace the existing DC$r\phi$ trigger. * SCS equivalent cost of rendered skilled manpower.

[4] M. Aivazis et al., Phys. Rev. **D50** (1994) 3102.
J. Collins, Phys. Rev. **D58** (1998) 094002.

[5] A. Martin et al., Eur. Phys. J. **C4** (1998) 463.
H. Lai et al., *hep-ph/9903282*, submitted to Eur. Phys. J.

[6] H1 Collaboration, S. Aid et al., Nucl. Phys. **B470** (1996) 3.
H1 Collaboration, C. Adloff et al., DESY **99-107**, submitted to Eur. Phys. J.

[7] V. Gribov, L. Lipatov, Sov. J. Nucl. Phys. **15** (1972) 438 & 675.
Yu. Dokshitzer, JETP **46** (1977) 641.
G. Altarelli, G. Parisi, Nucl. Phys. **B126** (1977) 298.

[8] E. Kuraev et al., *Sov. Phys. JETP* **45** (1977) 199.
Y. Balitsky, L. Lipatov, *Sov. J. Nucl. Phys.* **28** (1978) 822.
L. Lipatov, *Sov. Phys. JETP* **63** (1986) 904.

[9] H1 Collaboration, C. Adloff et al., Eur. Phys. J. **C1** (1998) 97.
H1 Collaboration, C. Adloff et al., DESY **98-205**, submitted to Eur. Phys. J.

[10] H1 Collaboration, C. Adloff et al., Z. Phys. **C76** (1997) 613.

[11] H1 Collaboration, Conference Paper 157ae, International Europhysics Conference on High Energy Physics, Tampere, Finland (1999).

[12] H1 Collaboration, Conference Paper 157ag, International Europhysics Conference on High Energy Physics, Tampere, Finland (1999).

[13] H1 Collaboration, C. Adloff et al., DESY **99-126**, submitted to Phys. Lett. B.

[14] H1 Collaboration, *Proposal for an Upgrade of the H1 Luminosity System and its Associated Electronics for HERA 2000*, Proposal submitted to the Physics Research Committee, PRC 98/05.

[15] H1 Collaboration, C. Adloff et al., DESY **99-010**, submitted to Eur. Phys. J.

[16] H1 Collaboration, C. Adloff et al., DESY **99-026**, submitted to Eur. Phys. J.

[17] H1 Collaboration, Conference Paper 574, 29th International Conference on HEP, Vancouver, Canada (1998).

[18] L. Frankfurt et al., Phys. Rev. **D54** (1996) 3194.
A. Martin et al., Phys. Rev. **D55** (1997) 4329.

[19] H1 Collaboration, Conference Paper 157aj, International Europhysics Conference on High Energy Physics, Tampere, Finland (1999).

[20] M. Tlucykont, *"z-Kalibration der zentralen Spurkammer des H1-Detektors bei HERA"*, diploma thesis, Universität Hamburg, Febr. 1999.

A Appendix A: Assumptions made for table 2

Assumptions for D^* decay (DIS)

- σ_{vis}: *Visible cross section to $K\pi\pi$ channel for selection criteria in [2].*
- **L1 conditions:** *SPACAL electron and multiple tracks (160 Hz). With the FTT, it may be possible to relax the strong L1 track condition and to require only a z-vertex trigger instead. The L1 rate would then be ~ 500Hz. The L2 and L3 rates would increase only slightly and the efficiency would improve by a small amount.*
- **L2 conditions:** *Cut on either electron energy or $\sum |pt|$ of tracks to obtain a rate reduction by a factor 5.*
- **L3 conditions:** *For $|m(K\pi) - m(D^*)| < 200$ MeV and $m(K\pi\pi_{\rm slow}) - m(K\pi) < 155$ MeV cuts, total reduction factor is approximately 30.*
- **FTT efficiency:** *Total efficiency (all three trigger levels) is assumed to be of the order of 70%.*
- **Efficiency without FTT:** *Assume L1 downscale by $1/160$ to achieve 1 Hz output. About 95% trigger efficiency without downscaling.*

Assumptions for D^* decay (γp)

- σ_{vis}: *Visible cross section to $K\pi\pi$ channel for selection criteria in [2].*
- **L1 conditions:** *Low angle tagged electron and multiple tracks (120 Hz) or require only a z-vertex trigger instead of multiple tracks (~ 500Hz).*
- **L2 conditions:** *Cut on $\sum |pt|$ of tracks to obtain a rate reduction by a factor 5.*
- **L3 conditions:** *For $|m(K\pi) - m(D^*)| < 200$ MeV and $m(K\pi\pi_{\rm slow}) - m(K\pi) < 155$ MeV cuts, total reduction factor is approximately 30.*
- **FTT efficiency:** *Total efficiency (all three trigger levels) is assumed to be of the order of 60%.*
- **Efficiency without FTT:** *Assume L1 downscale by $1/120$ to achieve 1 Hz output. About 85% trigger efficiency without downscaling.*

Assumptions for ρ production in DIS

- σ_{vis}: *Visible cross section for elastic* $\rho^0 \to \pi^+\pi^-$ *for selection criteria in [15].*
- **L1 conditions:** *Inclusive SPACAL trigger with high electron energy threshold, such that kinematics force decay pions into CJC.*
- **L2 conditions:** *Demand exactly two tracks.*
- **L3 conditions:** *Cut on invariant mass of* $\pi^+\pi^-$ *around* ρ *peak.*
- **FTT efficiency:** *Total trigger efficiency is assumed to be of the order of 80%*
- **Efficiency without FTT:** *L1 downscale by* $1/40$ *to achieve* 1 Hz *output. About 80% trigger efficiency without downscaling.*

Assumptions for elastic / inelastic J/Ψ

- σ_{vis}: *Visible cross sections for selection criteria in [16]. Visible cross sections for each of muon and electron channels are approximately* 500 pb *(elastic and quasi-elastic) plus* 500 pb *(inelastic).*
- **L1 conditions:** *Topological triggers for* e^+e^-*, muon triggers for* $\mu^+\mu^-$ *as currently used.*
- **L2 conditions:** *Cut on track with second highest* p_{t} *at 0.8 GeV.*
- **L3 conditions:** *Cut on invariant mass around the* J/ψ*;* 3 ± 0.5 GeV *to give* ~ 3 Hz*. For the elastic case, require in addition exactly two tracks to obtain rate* ~ 1 Hz*.*
- **FTT efficiency:** *Total trigger efficiency varies between approximately 12% (inelastic* e^+e^-*) and 60% (*$\mu^+\mu^-$*).*
- **Efficiency without FTT:** *L1 downscale by* $1/20$ *and use existing L2 topological / neural network trigger to achieve* 1 Hz *output. Total efficiency varies between* 15% *(inelastic* e^+e^-*) and* 70% *(*$\mu^+\mu^-$*) without downscaling.*

Assumptions for Υ

- σ_{vis}: *Visible cross section for selection criteria in [17] to* $\mu^+\mu^-$ *and* e^+e^- *channels.*
- **L1 conditions:** *Topological triggers for ee, muon triggers for* $\mu\mu$ *as currently used.*
- **L2 conditions:** *Cut on track with second highest* p_{t} *at 3.0 GeV.*
- **L3 conditions:** *Require dilepton invariant mass of at least 9 GeV to achieve* ~ 2 Hz*. For the elastic case, require in addition exactly 2 tracks to achieve* ~ 0.5 Hz*.*
- **FTT efficiency:** *Total trigger efficiency is assumed to vary between 12% (inelastic* e^+e^-*) and 60% (*$\mu^+\mu^-$*).*
- **Efficiency without FTT:** *L1 downscaled by* $1/20$ *and use existing L2 topological / neural network trigger to achieve* 1 Hz *output. Total efficiency varies between* 15% *(inelastic* e^+e^-*) and* 70% *(*$\mu^+\mu^-$*) without downscaling.*

Assumptions for W $\rightarrow \mu\nu$

- σ_{vis}: *Estimated visible cross section to $\mu\nu$ channel.*
- **L1 conditions:** *Muon triggers as currently operational.*
- **L2 conditions:** *Cut on the track with highest p_{t} at 10 GeV.*
- **L3 conditions:** *Applying isolation criterion on highest p_{t} track gives an estimated reduction of a factor 80 relative to the L1 rate.*
- **FTT efficiency:** *Total trigger efficiency is assumed to be of the order of 70%.*
- **Efficiency without FTT:** *L1 downscaled by $1/20$ to achieve $1\ \mathrm{Hz}$ output. Total trigger efficiency is about 75% based on track triggers alone without downscaling.*